Authors answer

We thank the editor for taking into consideration our paper for publication and the referees for the useful commentary provided. Any suggested corrections have been carefully examined and the corrected paper is presented with the following answers to the referees comments.
The main improvements brought to the paper are:

1) *Figure 1 has been modified to better show the rationale of the algorithm.*
2) *A more detailed illustration of the algorithm for the multivariate case has been provided in Section 2.2.*
3) *The minimum moving sum has been added as an indicator of the long-term dependence structure (Figure 7). The commentary to this result can be found in Section 4.4.*
4) *Section 3.1 "Imposing a trend" has been simplified and a commentary about the application of the technique has been added in section 4.2.*

Line numbering refers to the revised manuscript attached. The second file attached contains the tracking of the corrections.
We hope that the revised paper will be evaluated positively and we keep ourselves available for any further suggested improvements.

Best regards.
F.Oriani, J.Staubhaar, P.Renard and G.Mariethoz.

Anonymous Referee #1
General comments The discussion paper demonstrates a simple and robust data generation method that has not been widely applied in hydrology. Its application to daily rainfall generation therefore adds considerable value to stochastic hydrology and highlights the ability of non-parametric approaches for data generation. The methods applied are valid but some details are left out and it would be difficult for the reader to replicate the analysis. The discussion and conclusions reflect the analysis and results obtained. Specific comments Section 2.2 of the paper describes the Direct Sampling (DS) method and uses Figure 1 to illustrate the method. It is not clear exactly how SG is obtained. How different is ST from the historic record?

We understand that section 2.2 was unclear and we hope to have substantially improved it in the revision. The definition of SG has been elaborated in section 2.1 (lines 73-76) of the revised paper.

Is the value of t (in x(t)) get randomly obtained from a uniform distribution (Random[0,1]× length of simulated time series)?

Correct, the simulation order is randomly generated from a uniform distribution. This is now clarified in section 2.2, lines 103-104.

Figure 1 is not very informative and might be better if it illustrates a single or two iterations in chronological order.

We agree, figure 1 has been modified in order to better explain the copy-paste rule at the base of the algorithm.

Section 2.2 does not inform how auxiliary variables are used as part of the DS method. It seems that the search for Z(yi) continues until the thresholds for all the auxiliary variables are met but this is not stated in Section 2.2.

We agree, the procedure has now been clarified in section 2.2, lines 147-150.

It may be possible to get rid of patches (Section 3.2) by imposing a condition that the Z(yi) selected should not result in a patch in addition to its meeting the set thresh-
old of dissimilarity.

We think the suggested improvement can be a valid optional feature in cases where a total absence of patching is critical, and it will be considered in further work.
Nevertheless, for the application shown in the paper and the proposed setup, we do not see a real need for it since the observed patching is very low. We believe that in this case, forcing the algorithm to totally get rid of the patches is not going to bring an effective improvement to the simulation and may reduce the performance by over-conditioning. As shown in the results, the patching obtained is negligible when using the proposed setup together with an appropriate training dataset (i.e. sufficiently long with respect to the simulated time-series and with a low amount of gaps).
Moreover, as far as we have seen in the results of the tests conducted until now, the algorithm is not naturally prone to patching. A considerable patching is generally due to an inadequate parameterization or too limited/fragmented training dataset and results in a bad overall performance of the algorithm. The user is warned about these issues (Section 3 lines 208-211, 272-275). Therefore, in the most part if not all the cases in which a considerable patching occurs, a more efficient solution would be to find an opportune setup or training dataset instead of pushing the algorithm not to generate the patching itself.

In addition to the 10-years MS comparisons presented in Figure 6,
the minimum run sums for various lengths (up to say 10 or 20 years) could be used to assess how well DS replicates the long-term dependence characteristics of the rainfall.

We agree, the minimum moving average (the moving sum divided by the window length, which improves the visibility) with various windows up to 60 years has been computed for the stationary simulations (see fig.7) and a commentary has been added at lines 420-430.

Suggestion changes to sentence structure etc. Page 3214 line 13 . . .. reproduced adequately, reducing the . . .. . . Page 3214 line 23-24 . . .. Solutions to deal with this limitation . . .. Page 3215 line 12 . . ... completely capture a complex . . .. Page 320 line 2 . . ..event and acceptance threshold. . ... Page 3220 line 20-21 and other locations: should it be datum or data? Page 3222 line 7 Table 1 presents the dataset . . .. Page 3222 lines 14-15 Mariethoz and Renard (2010) show how direct sampling can be used for data reconstruction Page 3222 line 3 and page 3239: why is (*) included?

The training image includes the target and the auxiliary variables. To clarify this point, "" as been changed to "6"in Section 3 line 219 as well as Table 1.*

Page 3228 line 16: —- discussed in the following section. Page 3242 replace ‘ dotted line’ with ‘blue dots’

We agree with the suggestions, the revised paper has been changed accordingly.

Anonymous Referee #2

General comments:

The manuscript proposes the Direct Sampling (DS) technique to simulate daily rainfall data as an alternative to the parametric models. As this method resamples the data from the training image based on certain criteria, it cannot simulate values larger than the ones in the training image. Based on this one can say that this method is inferior to the other non-parametric methods such as Harrold et al. (2003b) and Mehrotra and Sharma (2007).

We agree with the referee, this limitation is put in evidence at line 374 and in the conclusions, line 486. On the other hand, the advantage of the DS with respect to the parametric techniques is the faithful reproduction of the time-dependence structure and distribution at higher scales, where also extremes higher than the reference are generated. Ongoing tests and a detailed comparison between the DS and the mentioned family of techniques will be the subject of a future publication.

Apart from this, the model adequately preserves the statistical characteristics of the historical data used in the simulation. The section on non-stationary simulation (Section 4.6) is not clear, confusing and not relevant to manuscript.

We think that the simplicity in which even a complex non-stationarity can be reproduced is a valuable and essential aspect of the algorithm and should be illustrated for time-series simulation, therefore we did not remove this part of the manuscript.
We agree about the lack of clarity: the explanation of the methodology has been simplified in Section 3.1 and the relevance of the application is now put in evidence at lines 467-470 .

I cannot understand why PACF was used to assess the correlation in the data. ACF should have been used in its place.

ACF and PACF are algebraically linked by the Yule-Walker equations (see for example [1] p.64) and contain the same information. Since here the aim was to investigate how efficiently each time-lag dependence is reproduced by the algorithm, the PACF has been chosen since it shows the linear dependence for each time-lag independently, which is not the case for the ACF. This is clarified at lines 335-340.

The manuscript should be revised before it can be published in HESS.

Specific comments:

The word "global" appears at a number of places and I cannot understand what it really means. Please explain.

We agree, the term is ambiguous, it has been changed to "marginal" referring to the probability distribution (lines 294,417,496).

PACF is not relevant and there is no need to calculate the correlations for lags up to 10 or 20.

Since the algorithm operates in a non-parametric way and imposes a variable time-dependence, the eventuality of modifying the persistence of the signal cannot be excluded a priori. That is why the daily PACF is calculated up to the 20th lag, just to show that no artifacts are introduced. This has been clarified at lines 440-443.
At the monthly scale a more complex dependence structure justifies the computation until the upper lags.

Technical corrections:
Page 3214, Line 13: Replace "exhaustively" with "well" or "satisfactorily" Page 3214, Line 23: Change "overtake" to "overcome" Page 3216, Lines 12-15: Sect 3 is missing. Sect 3 describes the application of the method. Page 3219, Line 17: Changed "informed" to "covered" Page 3219, Line 24: Change "respect" to "preserve" Page 3220, Line 5: Change "informed" to "selected" Page 3222, Line 5: Change "showing and extreme" to "showing an extreme" Page 3223, Line 4: Change "respect more strictly" to "preserve" Page 3223, Line 15: Change "showed" to "shown" Page 3224, Line 18: What is the statistics mentioned here? Page 3226, Line 16: Change "Another used validation criterion" to "Another validation criterion used " Page 3226, Line 17: Change "transformed in a" to "transformed into a" Page 3226, Line 19: Change "region" to "spell"

We agree with the suggestions, the revised paper has been changed accordingly

Page 3227, Lines 1 -24: PACF is not appropriate here. ACF should be used to assess the correlation with the well-known confidence limits. Delete lines 15 – 24.

We agree on the fact that the detailed explanation about the confidence limits is unnecessary, it has been deleted accordingly. The motivation for using PACF instead of ACF is explained above. Besides, the confidence limits are still valid for PACF since based on the autocorrelation of an IID ~ $N(0,\sigma^2)$, for which the two functions are statistically zero valued and equivalent (see [1] p.65).

Page 3229, Line 8: What is meant by "border"? Do the authors mean the start and end of the time series.

Correct, the term has been changed accordingly.

Page 3228, Line 16: Insert "section" after "following"
Page 3230, Lines 12-13: Not clear. Page 3230, Line 17: Change "respected" to "preserved"

We agree with the suggestions, the revised paper has been changed accordingly.

Page 3231, Lines 8-28: These can be deleted. There is no need to calculate the correlations up to 10 or 20 lags. Lag one correlation coefficient is adequate.

We agree on the fact that we do not expect a significant autocorrelation in the reference for lags greater than 1. The reason for computing that is explained above.

Besides, the model only cater for lag one correlation by considering the sum of current and previous day rainfall (2MS) as a covariate.

We do not agree, the 2MS is used to respect more accurately the lag-one autocorrelation, since we know a priori that it is the most important short-term dependence for daily rainfall. But it is not the sole lag the algorithm takes into account. As explained in Section 2.2 lines 136-143, higher order dependences are variably taken into account by the data event of the target variable, which changes size during the simulation. This concept has been clarified at lines 228-230.

Page 3232, Line 1: What is the non-stationarity imposed?

The non-stationarity is the one found in the TI. The sentence has been rewritten (line 456) to clarify this point.

Page 3232, Line 7: What is meant by "global" statistic? This word has been used at several places Page 3233, Line 21: Change "Goundwater" to "Groundwater"

We agree with the suggestions, the revised paper has been changed accordingly.

[1] Box, G. E. and Jenkins, G. M.: Time series analysis, control, and forecasting, Revised Edition, San Francisco, CA: Holden Day, 1976.

Manuscript prepared for Hydrol. Earth Syst. Sci.
with version 5.0 of the LaTeX class copernicus.cls.
Date: 24 June 2014

Simulation of rainfall time-series from different climatic regions using the Direct Sampling technique

F. Oriani[1], J. Straubhaar[1], P. Renard[1], and G. Mariethoz[2]

[1]Centre of Hydrogeology and Geothermics , University of Neuchâtel, Neuchâtel, Switzerland
[2]School of Civil and Environmental Engineering, University of New South Wales, Sydney, New South Wales

Correspondence to: Fabio Oriani
(fabio.oriani@unine.ch)

Abstract. The Direct Sampling technique, belonging to the family of multiple-point statistics, is proposed as a non-parametric alternative to the classical autoregressive and Markov-chain based models for daily rainfall time-series simulation. The algorithm makes use of the patterns contained inside the training image (the past rainfall record) to reproduce the complexity of the signal without inferring its prior statistical model: the time-series is simulated by sampling the training dataset where a sufficiently similar neighborhood exists. The advantage of this approach is the capability of simulating complex statistical relations by respecting the similarity of the patterns at different scales. The technique is applied to daily rainfall records from different climate settings, using a standard setup and without performing any optimization of the parameters. The results show that the overall statistics as well as the dry/wet spells patterns are simulated accurately. Also the extremes at the higher temporal scale are reproduced ~~exhaustively~~adequately, reducing the well known problem of over-dispersion.

1 Introduction

The stochastic generation of rainfall time-series is a key topic for hydrological and climate science applications: the challenge is to simulate a synthetic signal honoring the ~~high order~~ high-order statistics observed in the historical record, respecting the seasonality and persistence from the daily to the higher temporal scales. Among the different proposed techniques, exhaustively reviewed by Sharma and Mehrotra (2010), the most commonly ~~used~~ adopted approach to the problem ~~, adopted~~ since the '60 ~~,~~ is the Markov-chain (MC) simulation: in its classical form, it is a linear model which cannot simulate the variability and persistence at different scales. ~~Some recently adopted solutions to overtake this limit~~ Solutions to deal with this limitation consist of introducing exogenous

climatic variables and large-scale circulation indexes (Hay et al., 1991; Bardossy and Plate, 1992; Katz and Parlange, 1993; Woolhiser et al., 1993; Hughes and Guttorp, 1994; Wallis and Griffiths, 1997; Wilby, 1998; Kiely et al., 1998; Hughes et al., 1999), lower-frequency daily rainfall covariates (Wilks, 1989; Briggs and Wilks, 1996; Jones and Thornton, 1997; Katz and Zheng, 1999) or an index based on the short-term daily historical or previously generated record (Harrold et al., 2003a,b; Mehrotra and Sharma, 2007a,b) as ~~conditional~~ conditioning variables for the estimation of the MC parameters. By doing this, non-linearity is introduced in the prior model, the MC parameters changing in time as a function of some specific low-frequency fluctuations. An alternative proposed method is model nesting (Wang and Nathan, 2002; Srikanthan, 2004, 2005; Srikanthan and Pegram, 2009), that implies the correction of the generated daily rainfall using a multiplicative factor to compensate the bias in the higher-scale statistics. These techniques generally allow a better reproduction of the statistics up to the annual scale, but they imply the estimation of a more complex prior model and cannot completely ~~catch~~ capture a complex dependence structure.

In this paper, we propose the use of some lower-frequency covariates of daily rainfall in a completely unusual framework: the Direct Sampling (DS) technique (Mariethoz et al., 2010), which belongs to multiple-point statistics (MPS). Introduced by Guardiano and Srivastava (1993) and widely developed during the last decade (Strebelle, 2002; Allard et al., 2006; Zhang et al., 2006; Arpat and Caers, 2007; Honarkhah and Caers, 2010; Straubhaar et al., 2011; Tahmasebi et al., 2012), MPS is a family of geostatistical techniques widely used in spatial data simulations and particularly suited to pattern reproduction. MPS algorithms use a training image, i.e. a dataset to evaluate the probability distribution (pdf) of the variable simulated at each point (in time or space), conditionally to the values present in its neighborhood. In the particular case of the Direct Sampling, the concept of training image is taken to the limit by avoiding the computation of the conditional pdf and making a random sampling of the historical dataset where a pattern similar to the ~~conditional~~ conditioning data is found. If the training dataset is representative enough, these techniques can easily reproduce high-order statistics of complex natural processes at different scales. MPS has already been successfully applied to the simulation of spatial rainfall occurrence patterns (Wojcik et al., 2009). In this paper, we test the Direct Sampling on the simulation of daily rainfall time-series. The aim is to reproduce the complexity of the rainfall signal up to the decennial scale, simulating the occurrence and the amount at the same time with the aid of a multivariate dataset. Similar algorithms performing a multivariate simulation had been previously developed by Young (1994) and Rajagopalan and Lall (1999) using a bootstrap-based approach. As discussed in details in Section 2.3, the advantage of the Direct Sampling with respect to the mentioned techniques is the possibility to have a variable high-order time-dependence, without incurring excessive computation since the estimation of the n-dimensional conditional pdf is not needed. Moreover, we propose a standard setup for rainfall simulation: an ensemble of auxiliary variables and fixed values for the main parameters required by the Direct Sampling algorithm, suitable for the simulation of any stationary rainfall time-series,

without the need of calibration. The technique is tested on three time-series from different climatic regions of Australia. The paper is organized as follows: in Section 2 the DS technique ~~, the dataset used~~ is introduced and compared with the existing resampling techniques. The dataset used, the proposed setup and the method of evaluation are described in Section 3. The statistical analysis of the simulated time-series is presented and discussed in Section 4 and Section 5 is dedicated to the conclusions.

2 Methodology

In this section we recall the basics of multiple-point statistics and we focus on the Direct Sampling algorithm. The dataset used is then presented as well as the methods of evaluation.

2.1 Background on multiple-point statistics

Before entering in the details of the DS algorithm, let us introduce some common elements of MPS. The whole information used by MPS to simulate a certain process is based on the *Training Image* (TI) or *training dataset*: the dataset constituted of one or more variables used to infer the statistical relations and occurrence probability of any datum in the simulation. The TI may be constituted of a conceptual model instead of real data, but in the case of the rainfall time-series it is more likely to be a historical record of rainfall measurements. The *Simulation Grid* (SG) is a ~~totally or partially uninformed N-dimensional array~~ time referenced vector in which the ~~algorithm generates values to obtain the actual output of~~ generated values are stored during the simulation. ~~It usually has the same dimensionality as the training image. In the case of a rainfall time-series simulation~~ Following a simulation path which is usually random, the SG is ~~a time-referenced one-dimensional vector of random variables (referred to as one variable for the sake of simplicity), each of which represents the rainfall amount for a certain time-step~~progressively filled with simulated values and becomes the actual output of the simulation. The *conditioning data* ~~(CD)~~ are a group of given data (e.g. rainfall measurements) situated in the SG. Being already informed, no simulation occurs at those time-steps. The presence of ~~CD~~ conditioning data affects, in their neighborhood, the conditional law used for the simulation and limits the range of possible patterns. MPS, as well some MC based algorithm for rainfall simulation (see Section 1), may include the use of *auxiliary variables* to condition the simulation of the target variable. ~~An auxiliary variable is normally given as CD but, in the case of the Direct Sampling, it can also be~~ Auxiliary variables may either be known (fully or partially) and used to guide the simulation, or they may be unknown but still co-simulated ~~with the target, without being necessarily informed~~because their structures contains important characteristics of the signal. For rainfall time-series, it could be for example: covariates of the original or previously simulated data (e.g. the number of wet days in a past period), a correlated variable for which the record is known, a theoretical variable that imposes a periodicity or a trend (e.g. a sinusoid function describing the

annual seasonality over the data). Finally, the *search neighborhood* is a moving window, i.e. the portion of time-series located in the past and future neighborhood of each simulated value, used to retrieve the *data event*, i.e. the group of time-referenced values used to condition the simulation.

2.2 The Direct Sampling algorithm

Classical MPS implementations create a catalog of the possible neighbors patterns to evaluate the conditional probability of occurrence for each event with respect to the considered neighborhood. This may imply a significant amount of memory and always limits the application to categorical variables. On the contrary, the Direct Sampling generates each value by sampling the data from the TI where a sufficiently similar neighborhood exists. The DS implementation used in this paper is called *DeeSse* ~~software~~ (Straubhaar, 2011)~~, the~~ . The following is the main workflow of the algorithm ~~.~~ for the simulation of a single variable. For the multivariate case see the last paragraph of this section.

Let us denote $\boldsymbol{x} = [x_1, ..., x_n]$ the time vector representing the SG, $\boldsymbol{y} = [y_1, ..., y_m]$ the one representing the TI and $Z(\cdot)$ the target variable, object of the simulation, defined at each element of $\boldsymbol{x}$ and $\boldsymbol{y}$. Before the simulation begins, all continuous variables are normalized using the transformation $Z \longmapsto Z \cdot (max(Z) - min(Z))^{-1}$ in order to have distances (see step 3) in the range $[0, 1]$. During the simulation, ~~all the~~ the uninformed time-steps of the SG are visited in a random order. The random simulation path $t \in \{1, 2, ..., M\}$ is obtained by sampling without replacement the discrete uniform distribution $U(1, M)$ where M is the SG length. At each uninformed x_t, the following steps are executed:

1. The data event $\boldsymbol{d}(x_t) = \{Z(x_{t+h_1}), ..., Z(x_{t+h_n})\}$ is retrieved from the SG according to a fixed neighborhood of radius R centered on x_t~~it~~. It consists of at most N informed time-steps, closest to x_t. This defines a set of lags $H = \{h_1, ..., h_n\}$, with $|h_i| \leq R$ and $n \leq$ N. The size of $\boldsymbol{d}(x_t)$ is therefore limited by the user-defined parameter N and the available informed time-steps inside the search neighborhood.

2. A random time-step y_i in $\boldsymbol{y}$ is visited and the corresponding data event $\boldsymbol{d}(y_i)$, defined according to ~~the same~~ H, is retrieved to be compared with $\boldsymbol{d}(x_t)$.

3. A distance $D(\boldsymbol{d}(x_t), \boldsymbol{d}(y_i))$, i.e. a measure of dissimilarity between the two data events, is calculated. For categorical variables (e.g. the dry/wet rainfall sequence), it is given by the formula:

$$D(\boldsymbol{d}(x_t), \boldsymbol{d}(y_i)) = \frac{1}{n} \sum_{j=1}^{n} a_j, \qquad a_j = \begin{cases} 1 \; if \; Z(x_j) \neq Z(y_j) \\ 0 \; if \; Z(x_j) = Z(y_j) \end{cases} \tag{1}$$

while for continuous variables the following one is used:

$$D(\boldsymbol{d}(x_t), \boldsymbol{d}(y_i)) = \frac{1}{n} \sum_{j=1}^{n} |Z(x_{t_j}) - Z(y_j)| \tag{2}$$

where n is the number of elements of the data event. The ~~neighbors~~ elements of $\boldsymbol{d}(x_t)$, independently from their position, play an equivalent role in conditioning the simulation of $Z(x_t)$. Note that, using the above distance formulas, the normalization is not needed for categorical variables, while for the continuous ones it ensures distances in $[0, 1]$.

4. If $D(\boldsymbol{d}(x_t), \boldsymbol{d}(y_i))$ is below a fixed threshold T, i.e. the two data events are sufficiently similar, the iteration stops and the datum $Z(y_i)$ is assigned to $Z(x_t)$. Otherwise, the process is repeated from point 2 until a suitable candidate $\boldsymbol{d}(y_i)$ is found or the prescribed TI fraction limit F is scanned.

5. If a TI fraction F has been scanned and the distance $D(\boldsymbol{d}(x_t), \boldsymbol{d}(y_i))$ is above T for each visited y_i, the datum $Z(y_i^*)$ minimizing this distance is assigned to $Z(x_t)$.

This procedure is repeated for the simulation at each x_t until the entire SG is ~~informed~~covered. Figure 1 illustrates the iterative simulation using the Direct Sampling and stresses some of its peculiarities. First, simulating $Z(x_t)$ in a random order allows $\boldsymbol{x}$ to be progressively populated at non-consecutive time-steps. Therefore, the simulation at each x_t can be conditioned on both past and future, as opposed to the classical Markov-chain techniques, that use a linear simulation path starting from the beginning of the series, allowing conditioning on past only.

FIG.1 ABOUT HERE

In the early iterations, the closest informed time-steps used to condition the simulation are located far from x_t and its number is limited by the search window, i.e. conditioning is mainly based on large past and future time lags. On the contrary, the final iterations dispose of a more populated SG, conditioning is thus done on small time lags since only the closest N values are considered. This variable time-lag principle may not respect the autocorrelation on a specific time-lag rigorously, but it should ~~reproduce~~ preserve a more complex statistical relationship, which cannot be explored exhaustively using a fixed-dependence model.

The DS can simulate multiple variables together similarly to the univariate case, ~~but using a multivariate dataset as TI. In this case, we have~~ dealing with a vector of variables $\boldsymbol{Z}(x_t)$ ~~defined at each time step. point~~ and considering a data event $\boldsymbol{d}_k$ different for each k-th variable, defined by N_k and R_k. Unlike the implementation presented in (Mariethoz et al., 2010), *DeeSse* also uses a specific acceptance threshold T_k for each variable. Point 3 of the algorithm is ~~therefore repeated for each variable using an independent data event and acceptation threshold. It has to be remarked~~ repeated until a candidate with a distance below the threshold for all variables is found. If this condition is not met, the scan stops at the prescribed TI fraction F and the error for each candidate y_i and k-th variable is computed with the following formula: $E_k(y_i) = (D(\boldsymbol{d}_k(x_t), \boldsymbol{d}_k(y_i)) - \mathrm{T}_k)\mathrm{T}_k^{-1}$, where $D(\cdot, \cdot)$ is defined as in Point 3. Finally, the candidate minimizing $max(\boldsymbol{E}(y_i))$ is assigned to $\boldsymbol{Z}(x_t)$. Note that the entire data vector $\boldsymbol{Z}(x_t)$ is simulated in one iteration, reproducing exactly

the same combination of values found for all the variables at the sampled time-step, ~~excluded the already informed ones (conditioning data)~~excluding the conditioning data, already present in the SG. This feature, although reducing the variability in the simulation, has been adopted to accurately reproduce the correlation between variables~~accurately~~.

2.3 Comparison with existing resampling techniques

The resampling principle is at the base of some already proposed techniques for rainfall and hydrologic time-series simulation. There exist two principal families of resampling techniques: the block bootstrap (Vogel and Shallcross, 1996; Srinivas and Srinivasan, 2005; Ndiritu, 2011), which implies the resampling with replacement of entire pieces of time-series with the aim of preserving the statistical dependence at a scale minor than the blocks size, and the k-nearest neighbor bootstrap (k-NN), based on single value resampling using a pattern similarity rule. This latter family of techniques, introduced by Efron (1979) and inspired to the jackknife variance estimation, has seen several developments in hydrology (Young, 1994; Lall and Sharma, 1996; Lall et al., 1996; Rajagopalan and Lall, 1999; Buishand and Brandsma, 2001; Wojcik and Buishand, 2003; Clark et al., 2004). Having different points in common with the Direct Sampling, its general framework is briefly presented in the following. Each datum inside the historical record is characterized by a vector $\boldsymbol{d}_t$ of predictor variables, analogous to the data event for the DS. For example, to generate $Z(x_t)$ one could use $\boldsymbol{d}_t = [Z(x_{t-1}), Z(x_{t-2}), U(x_t), U(x_{t-1})]$, meaning that the simulation is conditioned to the 2 previous time-steps of Z and the present and previous time-steps of U, a correlated variable. In the predictor variables space $\mathbb{D}$, the historical data as well as $Z(x_t)$, which still has to be generated, are represented as points whose coordinates are defined by $\boldsymbol{d}_t$. Consequently, proximity in $\mathbb{D}$ corresponds to similarity of the conditioning patterns. $Z(x_t)$ is simulated by sampling an empirical pdf constructed on the k points closest to $Z(x_t)$; the closer the point is, the higher is the probability to sample the corresponding historical datum. Proposed variations of the algorithm include transformations of the predictor variables space, the application of kernel smoothing to the k-NN pdf to increase the variability beyond the historical values, and different methods to estimate the parameters of the model, e.g. k and the kernel bandwidth.

Going back to the Direct Sampling, the similarities with the k-NN bootstrap are: i) they both make a resampling of the historical record conditioned by an ensemble of auxiliary/predictor variables; ii) they both compute a distance as a measure of dissimilarity between the simulating time-step and the candidates considered for resampling. Nevertheless, there are several points of divergence in the rationale of the techniques: i) in the k-NN bootstrap, the distance is used to evaluate the resampling probability, while in the DS it is used to evaluate the resampling possibility. This means that, using the k-NN resampling, the conditional pdf is a function of the distance, while in the DS the distance is only used to define its support. In fact, using the DS, the space $\mathbb{D}$ is not restricted to the k nearest neighbors but it is bounded by the distance thresholds: outside the boundary, the

resampling probability is zero, while inside, it follows the occurrence of the data in the scanned TI fraction, without being a function of the pattern resemblance. Only in case of no candidate found, the closest neighbor outside the bounded portion of $\mathbb{D}$ is chosen for resampling. The latter can be considered as an exceptional condition which usually does not lead to a good simulation and seldom occurs using an appropriate setup and training dataset. ii) Using the DS, the conditional pdf remains implicit, its computation is not needed: the historical record is randomly visited instead and the first datum presenting a distance below the threshold is sampled. This is an advantage since it avoids the problem of the high-dimensional conditional pdf estimation which limits the degree of conditioning in bootstrap techniques (Sharma and Mehrotra, 2010). iii) The k-NN technique considers a fixed time-dependence, while it varies during the simulation in the case of the DS. iv) Finally, the simulation path (in the SG) is always linear in the k-NN technique, while it is random using the DS, allowing conditioning on future time-steps of the target variable.

3 Application

The dataset chosen for this study is composed of three daily rainfall time-series from different climatic regions of Australia: Alice Springs (hot desert), with a very dry rainfall regime and long droughts, Sydney (temperate), with a far wetter climate due to its proximity to the ocean, and Darwin (tropical savannah), showing ~~and~~ an extreme variability between the dry and wet seasons.

TAB.1 ABOUT HERE

Table 1 ~~delineates~~ presents the dataset used: the chosen stations ~~present~~ provide a considerable record of about 70 years for Darwin and Alice Springs and 150 years for Sydney. Any gaps or trends have been explicitly kept to test the behavior of the algorithm with incomplete or non-stationary datasets. The Direct Sampling treats gaps in the time-series in a simple way: each data event found in the TI is rejected if it contains any missing data. This allows incomplete training images to be dealt with in a safe way, but, as one could expect, a large quantity of missing data, especially if sparsely distributed, may lead to a poor simulation. ~~About dataset reconstruction using the direct sampling see~~ Mariethoz and Renard (2010) show how the Direct Sampling can be used for data reconstruction.

Since rainfall is a complex signal exhibiting not only multi-scale time dependence but also intermittence, the classical approach is to split the daily time-series generation in two steps: the occurrence model, where the dry/wet daily sequence is generated using a Markov-chain, and the amount model, where the rainfall amount is simulated on wet days using an estimation of the conditional pdf (e.g., Coe and Stern, 1982). The simulation framework proposed here is radically different: we use the Direct Sampling to generate the complete time-series in one step, simulating multiple variables together. In particular, the TI used is ~~composed of~~ based on the past daily rainfall record ~~(*) and the following auxiliary~~ and composed of the following variables (Table 2): 1) the average rainfall

amount on a 365 days centered moving window ($365MA$) [mm], 2) the sum of the current and the previous day amounts ($2MS$) [mm], 3) and 4) two out-of-phase of triangular functions ($tr1$ and $tr2$) with frequency 365.25 days, similar to trigonometric coordinates expressing the position of the day in the annual cycle, 5) the dry/wet sequence, i.e. a categorical variable indicating the position of a day inside the rainfall pattern (1 = wet, 0 = dry, 2 = solitary wet, 3 = wet day at the beginning or at the end of a wet spell), 6) the daily rainfall amount, which is the target of the simulation. The first two auxiliary variables are covariates used to force the algorithm to ~~respect more strictly~~ preserve the inter-annual structure and the day-to-day correlation, which are known to exist a priori. The other ones are used to reproduce the dry/wet pattern and the annual seasonality accurately. Moreover, any unknown dependence in the daily rainfall signal is generically taken into account in the simulation by using a data event of variable length as explained in Section 2.2. It has to be remarked that, apart from 3) and 4), which are known deterministic functions imposed as ~~CD~~conditioning data, the rest of the auxiliary variables are transformations of the rainfall datum, automatically computed on the TI and co-simulated with the daily rainfall.

To summarize, the main parameters of the algorithm are the following: the maximum scanned TI fraction F $\in (0,1]$, the search neighborhood radius R, the maximum number of neighbors N, both expressed in number of elements of the time vector, and the distance threshold T $\in (0,1]$. Recall that, apart from F, each parameter is set independently for each simulated variable. The setup shown in Table 2 is used together with F $= 0.5$ and proposed as a standard for daily rainfall time-series. A sensitivity analysis, not ~~showed~~ shown here, confirmed the generality of this setup which is not the result of a numerical optimization on a specific dataset, but it is rather in accordance to the criteria used to define the order and extension of the variable time-dependence, as shown below. Applying it to any type of single-station daily rainfall dataset, the user should obtain a reliable simulation without needing to change any parameter or give supplementary information. An additional refinement of the setup is also possible, keeping in mind the following general rules:

- R limits the maximum time-lag dependence in the simulation and should be set according to the length of the largest sufficiently repeated structure or frequency in the signal that has to be reproduced. Being interested to condition the simulation upon the inter-annual fluctuations (visible in the 10-years MA time-series in Figure 9), we set $\mathrm{R}_{365MS} = \mathrm{R}_{rainfall} = 5000$ for the $365MS$ and daily rainfall variables. We recommend keeping R below the half of the training dataset total length, to condition on sufficiently repeated structures only. Regarding dry/wet pattern conditioning, we prefer limiting the variable time dependence within a 21-days window ($\mathrm{R}_{dw} = 10$). ~~In general R_{dw}~~ This window should be set between the median and the maximum of the wet spell length distribution, in order to properly catch the continuity of the rainfall events over multiple days.

- N controls the complexity of the conditioning structure but also influences the specific time-lag dependence. For instance, if one increases N, higher-order dependencies are represented, but

the weight accorded to a specific neighbor in evaluating the distance between patterns becomes lower. This leads to a less accurate specific time-lag conditioning, but a more complex time-dependence is respected on average. For the rainfall amount and $365MA$ variables, $\mathrm{N} \ll \mathrm{R}$ follows the same setup rule as for R_{dw}. In this way, in the initial iterations, the conditioning neighbors will be sparse in a 10001 days window ($R = 5000$) to respect low-frequency fluctuations, whereas, in the final iterations, they will be contained in a N-days window to respect the within-spell variability. The standard value proposed here ($\mathrm{N}_{365MA} = \mathrm{N}_{365MA} = 21$) corresponds approximately to the spell distribution median of the Darwin time-series, remaining in the appropriate range for the other considered climates. Conversely, N_{dw} is kept lower in order to focus the conditioning on the small-scale dry/wet pattern. $\mathrm{N}_{dw} = 5$ gave in general the best result in terms of dry/wet pattern reproduction~~, with a gradual degradation of the statistics departing from this value~~.

- ~~The combination N = R = 1 for the~~ For $2MS$ ~~and tr auxiliary variables is equivalent to a lag-$(0,1)$ dependence and~~ , $tr1$ and $tr2$, the time-dependence is limited to lag 1 by using $\mathrm{N} = \mathrm{R} = 1$. This combination should not be changed since we have no interest in expanding or varying the time lag-dependence ~~in this case~~for the mentioned variables.

- T determines the tolerance in accepting a pattern. The sensitivity analysis done until now on different types of heterogeneities (Meerschman et al., 2013) confirmed that the optimum generally lies in the interval $[0.01, 0.07]$ (1 to 7% of the total variation). Higher T values usually lead to poorly simulated patterns~~and~~ , but lower ones may induce a bias in the ~~global statistics~~ marginal distribution and increase the phenomenon of verbatim copy, i.e. the exact reproduction of an entire portion of data by oversampling the same pattern inside the TI. For these reasons, we recommend keeping the proposed standard value $T = 0.05$ for all the variables.

- F should be set sufficiently high to have a consistent choice of patterns but a value close to 1, i.e. all the TI is scanned each time, may lower the variability of the simulations and increase the verbatim copy. Using a training dataset representative enough, the optimal value corresponds to a TI fraction containing some repetitions of the lowest-frequency fluctuation that should be reproduced. Considering the randomness of the TI scan, the value $\mathrm{F} = 0.5$ chosen in this paper is sufficient to serve the purpose.

TAB.2 ABOUT HERE

3.1 Imposing a trend

~~The~~ As already shown in (Chugunova and Hu, 2008; Mariethoz et al., 2010; Honarkhah and Caers, 2010; Hu et al., 2014), in case of a non-stationary target variable, the simulation can be constrained

to reproduce the same type of trend found in the TI by making use of an auxiliary variable ~~. The auxiliary variable proposed here for any type of non-stationarity is $L(y_t) = y_t$, corresponding to the TItime vector. An exact copy $L(x_t) = L(y_t)$ is present in~~ . The one proposed here is the integer vector $L = [1, 2, ..., \mathrm{M}]$, where M is the length of the time-series, tracking the position of each datum inside the TI. L is assigned to the SG as conditioning ~~data. The parametersfor $L(\cdot)$ are set as follows~~datum with the following parameters: $\mathrm{R}_L = 1$, $\mathrm{N}_L = 1$ and $\mathrm{T}_L = 0.01$. ~~Therefore~~According to the threshold T_L, the sampling ~~for each simulated datum $Z(x_t)$ is forced to remain inside the time neighborhood $I(x_t) = y_t \pm \mathrm{T}_L V(L)$, $V(L)$ being the total variation of L, i.e. the total length of the series. For example, for~~ is therefore constrained to a neighborhood of the same time-step inside the TI: for example, in the Darwin case, being ~~$V(L) = 26356$~~ $\mathrm{M} = 26356$ and $\mathrm{T}_L = 0.01$ (1% of the total variation allowed), the sampling to simulate $Z(x_t)$ is constrained to ~~$I(x_t) \approx y_t \pm 263$~~ the interval $y_t \pm 263$ [days]. In this way, the ~~main statistics are~~ marginal distribution is respected, but the local variability is ~~almost completely~~ restricted to the one found inside the training dataset, reproducing the ~~non stationarity~~same trend. The following remarks are noteworthy: i) ~~any type of non-stationarity is automatically imposed by L but, to properly catch the trend and~~ to avoid an unnecessary restriction ~~to the local variability, I should be equal~~ of the sampling, T_L should correspond to the maximum time interval for which the target variable can be considered stationary; ii) the simulation ~~cannot~~ should not be longer than the training dataset, having no basis to extrapolate the trend in the past or future; iii) the local variability is not completely limited by L: a pattern outside the tolerance range (i.e. with a distance over the threshold) could be sampled if no better candidate is found.

3.2 Validation

~~To validate~~ To test the proposed technique the visual comparison of the generated time-series with the reference as well as several groups of statistical indicators are considered. The empirical cumulative probability distributions, obtained using the Kaplan-Meier estimate (Kaplan and Meier, 1958), of the daily, the annual and decennial rainfall time-series, obtained by summing up the daily rainfall, are compared using quantile-quantile (qq-) plots. Moreover, the minimum moving average, i.e. the minimum value found on the moving average of each time-series, is computed using different running window lengths up to 60 years to assess the efficiency of the algorithm in preserving the long-term dependence characteristics of the rainfall.

The daily rainfall statistics have been analyzed separately for each month considering the average value of the following indicators: the probability of occurrence of a wet day and the mean, standard deviation, minimum and maximum on wet days only. For instance, the standard deviation is computed on the wet days of each month of January, then the average value is taken as representative of that time-series. We therefore obtain a unique value for the reference and a distribution of values for the simulations represented with a box-plot.

Another used validation criterion is the comparison of the dry and wet spells length distributions. Each series is transformed ~~in~~ into a binary sequence with zeros corresponding to dry days and ones to the wet days. Then, counting the number of days inside each dry and wet ~~region~~spell, we obtain the distributions of dry and wet spells length, that can be compared using qq-plots. This is an important indicator since it determines, for example, the efficiency of the algorithm in reproducing long droughts or wet periods.

Since the DS works by pasting values from the TI to the SG, it is straightforward to keep track of the original location of each value in the training image. If successive values in the TI are also next to each other in the SG, then a patch is identified. A multiple box-plot is then used to represent the number of patches found in each realization as a function of the patch length to keep track of the verbatim copy effect.

The last group of indicators considered is the sample Partial Autocorrelation Function (PACF) (Box and Jenkins, 1976) of the daily, monthly and annual rainfall. Given a time-series $\boldsymbol{X}_t$, the sample PACF is the estimation of the linear correlation index between the datum at time t and the ones at previous time-steps $t-h$, without considering the linear dependence with the in-between observations. For a stationary time-series the sample PACF is expressed as a function of the time-lag h with the following formula:

$$\hat{\rho}(X_t,h) = Corr[X_t - \hat{E}(X_t|\{X_{t-1},...,X_{t-h+1}\}), X_{t-h} - \hat{E}(X_{t-h}|\{X_{t-h+1},...,X_{t-1}\})] \quad (3)$$

where $\hat{E}(X_t|\{X_{t-1},...,X_{t-h+1}\})$ is the best linear predictor knowing the observations $\{X_{t-1},...,X_{t-h+1}\}$. $\rho(h)$ varies in $[0,1]$, with high values for a highly autocorrelated process. This indicator is widely used in time-series analysis since it gives information about the persistence of the signal. The autocorrelation function could be used instead, but PACF is preferred here since it shows the autocorrelation at each lag independently. In the case of daily rainfall, the partial autocorrelation is usually very low, while the higher-scale rainfall may present a more important specific time-lag linear dependence. As ~~suggested by ,~~ usually done in the absence of any prior knowledge about ~~$\boldsymbol{X}_t$, an accurate way to detect a significant autocorrelation at a certain lag, is to compare it with an IID $\sim N(0,\sigma^2)$ noise. Such a signal is totally non-autocorrelated and presents a sample PACF ($\hat{\rho}_{AN}$) near zero for any $h>1$. Moreover, $\hat{\rho}_{AN}$ follows the asymptotic normal distribution $AN(0,n^{-1})$, n being the number of observations in the considered sample. The 95% confidence interval of this distribution can be used to test~~ X_t, the $5-95\%$ confidence limits of an uncorrelated white noise are adopted to assess the significance of ~~any $\hat{\rho}(h)$. That is, in the estimation of the autocorrelation for $\boldsymbol{X}_t$, at all the $\hat{\rho}(h)$ values within $0 \pm 1.96n^{-1/2}$ can be considered negligible, being of the same magnitude as $\hat{\rho}_{AN}$. Conversely, the values outside these boundaries are probably the expression of a significant autocorrelation and should be reproduced by the simulation. The fact that the variance of $\hat{\rho}_{AN}$ as well as the size of the 95% confidence interval increase with n^{-1}, allows a correct PACF evaluation with respect to the limited information given by the considered sample.~~

the PACF indexes. Since the time-series used in this paper are not necessarily stationary, any sample PACF is computed from the standardized signal X_t^s, obtained by applying moving average estimation $\hat{m}_t$ and standard deviation $\hat{s}_t$ filters with the following formula:

$$X_t^s = \frac{X_t - \hat{m}_t}{\hat{s}_t}, \qquad \hat{m}_t = (2q+1)^{-1} \sum_{j=-q}^{q} X_{t+j}, \qquad \hat{s}_t = [(2q+1)^{-1} \sum_{j=-q}^{q} (X_{t+j} - \hat{m}_t)^2]^{-\frac{1}{2}}, \qquad q+1 \leq t \leq n-q \tag{4}$$

where $q = 2555$ (15 years centered moving window). It is important to note that this operation may exclude from the PACF computation a consistent part of the signal ($q+1 \leq t \leq n-q$), especially on the higher time-scale~~signal~~. In the case of the datasets used, the annual time-series is reduced to less than 60 values for Alice Springs and Darwin: a barely sufficient quantity, considering that ~~a generic~~ the minimum amount of data for a useful sample PACF estimation ~~given~~ suggested by Box and Jenkins (1976) is of about 50 observations.

4 Results and discussion

To evaluate the proposed technique, a group of 100 realizations of the same length as the reference is generated for each of the 3 considered datasets to obtain a sufficiently stable response in both the average and the extreme behavior. The setup used is the one presented in Section 3 with the fixed parameters values shown in Table 2. The obtained results are shown and discussed in the following section.

4.1 Visual comparison

Figure 2 shows the comparison between random samples from both the simulated and the reference time-series. For each dataset, the generated rainfall looks similar to the reference: the extreme events inside the 10-years samples are reproduced with an analogous frequency and magnitude. The annual seasonality, particularly pronounced in the Darwin series, is accurately simulated as well as the persistence of the rainfall events, visible in the 100-days samples. These aspects are evaluated quantitatively in the following sections.

FIG.2 ABOUT HERE

4.2 Multiple-scale probability distribution

The qq-plots of the rainfall empirical distributions are presented in Figure 3, where all the range of quantiles is considered. The distribution of the daily rainfall (computed on wet days only) is generally respected, although some extremes that are present only once in the reference and, in particular, at the ~~border~~ start or end of the time-series, may not appear in the simulation. It is the case of the Darwin series, with a mismatch of the very upper quantiles. Moreover, the DS being an

algorithm based on resampling, the distribution of the simulated values is limited by the range of the training dataset: this is shown in the Alice Springs and Sydney qq-plots, where the distribution of the last quantiles is clearly truncated at the maximum value found in the reference. This result is normally expected using this type of techniques: the direct sampling is of course not able to extrapolate extreme intensities higher than the ones found in the TI at the scale of the simulated signal.

FIG.3 ABOUT HERE

On the contrary, the distribution of the rainfall amount on the solitary wet days is accurately respected, with some realizations including higher extremes than the reference. More importantly, the annual and 10-years rainfall distributions are correctly reproduced and do not show over-dispersion. This phenomenon, common among the classical techniques based on daily-scale conditioning, consists in the scarce representation of the extremes and underestimation of the variance at the higher scale. This problem is avoided here because a variable dependence is considered, up to a 5000-days radius on the $365MA$ auxiliary variable, that helps ~~respecting~~ preserving the low-frequency fluctuations. We also see that, at this scale, the DS is capable of generating extremes higher than the ones found in the reference, meaning that new patterns have been generated using the same values at the daily scale. This results is purely based on the reproduction of higher-scale patterns: the acceptance threshold value chosen for the $365MA$ auxiliary variable allows enough freedom to generate new patterns although maintaining an unbiased distribution. Nevertheless, this approach is not meant to replace a specific technique to predict long recurrence-time events at any temporal scale, since it is not focused on modeling the tail of the probability distribution.

4.3 Annual seasonality and extremes

Figure 4 shows the principal indicators describing the annual seasonality of the reference and the generated time-series: each different season is accurately reproduced by the algorithm, with almost no bias. The probability of having a wet day, usually imposed by a prior model in the classical parametric techniques, is indirectly obtained by sampling from the rainfall patterns of the appropriate period of the year. This goal is mainly achieved using the auxiliary variables $tr1$ and $tr2$ as ~~CD~~ conditioning data (see Section 3).

FIG.4 ABOUT HERE

~~Regarding the~~ The simulation of the average extremes, shown in Figure 5, ~~there is a more accurate simulation of the maxima with respect to the minima, slightly underestimated in the Sydney series~~also follows the reference rather accurately.

FIG.5 ABOUT HERE

4.4 Rainfall patterns and verbatim copy

The statistical indicators regarding the dry/wet patterns shown in Figure 6 demonstrate the efficiency of the proposed DS setup in simulating long droughts or wet periods according to the training dataset: the dry and wet spells distributions are ~~respected~~ preserved and extremes higher than the ones present in the TI are also simulated.

The verbatim copy box-plots show the distribution of the time-series pieces exactly copied from the TI as a function of their size for the ensemble of the realizations: the number of patches decreases exponentially with their size. The phenomenon is mainly limited to a maximum of few 8-days patches, with isolated cases up to 14 days.

The 10-years rainfall moving sum, shown at the bottom of Figure 6, ~~shows~~ illustrates the low-frequency time-series structure: the quantiles of the simulations at each time-step confirm that the ~~global~~ overall variability is correctly simulated, but the local fluctuations ~~and global trends~~ do not match the reference. For example, the Darwin reference series shows a clear upward ~~global tendency~~ trend which is not present in the superposed randomly-picked DS realization. Generally, the TI is supposed to be stationary or the non-stationarity should be at least described by an auxiliary variable. If it is not the case, as for the Darwin time-series, the algorithm ~~respects the global variation~~ honors the marginal distribution of the reference, but it does not reproduce a specific trend. This problem is treated separately in Section 4.6.

FIG.6 ABOUT HERE

The minimum moving average on different window lengths up to 60 years (Figure 7) gives information about the long-term structure of rainfall. The zero values are in accordance with the dry spell distribution shown in Figure 6: for example, Alice Springs presents a zero minimum moving average until 5 months, meaning that it contains dry spells of this length. Alice Springs and Sydney show a very different long-term structure: the former with long dry spells, the latter with a wider range of minimum values. Darwin presents the peculiarities of both climates with a sharp rising from the annual to the 60 years scale.

FIG.7 ABOUT HERE

According to this indicator, the simulation of the long-term structure is fairly accurate. The negative bias, lower than 0.5 mm, shows a modest tendency to underestimate the minimum moving average from the annual to the decennial scale for wet climates as Sydney and Darwin.

4.5 Linear time-dependence

The specific linear time-dependence of the generated and reference ~~signal~~ signals has been evaluated at different scales using the sample Partial Autocorrelation Function (PACF, Figure ~~??~~8, Equation 4).

FIG.~~??~~ 8 ABOUT HERE

At the daily scale, the data show the same level of autocorrelation at lag-1 and a low but significant linear dependence until lag 3 for Alice Springs and Sydney, while Darwin presents a longer tailing which asymptotically approaches the confidence bounds of ~~the Gaussian~~ an uncorrelated noise. The DS simulation shows a tendency to a slight underestimation of the lag-1 PACF, with a maximum error around 0.1 ~~(the Sydneytime-series). The rest of the lags are reproduced quite accurately~~for Sydney. Since the algorithm operates in a non-parametric way and imposes a variable time-dependence, the eventuality of modifying the structure of the daily signal cannot be excluded a priori, for this reason the PACF has been calculated up to the 20th lag, assuring that no extra linear-dependence has been introduced.

At the monthly scale, the linear time-dependence structure is clearly related to the annual seasonality, with a negative autocorrelation around lag 6 and a positive one around lag 12. The climate characterization is also evident: from Alice Springs to Darwin we see a more marked seasonality reflected in the PACF. The simulation follows the reference fairly well, with a maximum error around ± 0.1.

At the annual scale, the limited length of the time-series ~~reduces~~ leads to wider confidence bounds for the non-significant values (see section 3.2). The reference does not show a clear linear time-dependence structure which is not similarly reproduced by the simulation. Some more relevant discrepancy is present in the Darwin series, ~~presenting~~ showing a more discontinuous structure. However, using such a limited dataset for the time scale considered here, it is difficult to determine if the reference PACF is really indicative of an effective linear dependence.

4.6 Non-stationary simulation

Figure 9 shows the Darwin time-series simulation ~~realized by imposing~~ preserving the same non-stationarity ~~with~~ contained in the reference by using the technique proposed in Section 3.1. The 10-years moving sum plot shows that the ~~local and global trend of~~ trend and low-frequency fluctuation present in the reference are accurately ~~reproduced~~simulated: the median of the realizations follows the reference and a variability of about 4 ~~m~~ m between the 5-th and 95-th percentile is present. ~~The accuracy in the global statistics~~ Regarding the other considered statistical indicators, the performance appears to be essentially the same as for the stationary simulation: the only remarkable difference is a modest positive bias in the maximum wet periods length.

FIG.9 ABOUT HERE

The fact that, to impose the trend, the sampling is restricted to a local region of the reference reduces the local variability with respect to the stationary simulation. Consequently, a ~~little~~ modest increase of the verbatim copy effect occurs.

This technique can find application in cases where a specific non-stationarity extended to high-order moments should be imposed, e.g. exploring the uncertainty of a given past or future scenario, where a simple trend or seasonality adjustment is insufficient and an overly complex parametric model would be necessary to preserve the same long-term behavior.

5 Conclusions

The aim of the paper is to present an alternative daily rainfall simulation technique based on the Direct Sampling algorithm, belonging to multiple-point statistics family. The main principle of the technique is to resample a given dataset using a pattern-similarity rule. Using a random simulation path and a non-fixed pattern dimension, the technique allows imposing a variable time-dependence and reproducing the reference statistics at multiple scales. The proposed setup, suitable for any type of rainfall, includes the simulation of the daily rainfall time-series together with a series of auxiliary variables including: a categorical variable describing the dry/wet pattern, the 2 days moving sum which helps respecting the lag-1 autocorrelation, the 365 days moving average to condition upon inter-annual fluctuations and two coupled theoretical periodic functions describing the annual seasonality. Since all the variables are automatically computed from the rainfall data, no additional information is needed.

The technique has been tested on three different climates of Australia: Alice Springs (desert), Sydney (temperate) and Darwin (tropical savannah). Without changing the simulation parameters, the algorithm correctly simulates both the rainfall occurrence structure and amount distribution up to the decennial scale for all the three climates, avoiding the problem of over-dispersion, which often affects daily-rainfall simulation techniques. Being based on resampling, the algorithm can only generate data which are present in the training dataset, but they can be aggregated differently, simulating new extremes in the higher-scale rainfall and dry/wet pattern distributions. The technique is not meant to be used as a tool to explore the uncertainty related to long recurrence-time events, but rather to generate extremely realistic replicates of the datum, to be used as inputs in hydrologic models.

Reproducing ~~a trend in the simulation~~ the specific trend found in the data is also possible by making use of an additional auxiliary variable which simply restricts the sampling to a local portion of the TI. This way, any type of non-stationarity present in the TI is automatically imposed on the simulation. The Darwin example demonstrates the efficiency of this approach in reproducing 100 different realizations showing the same type of trend and ~~global statistics~~marginal distribution. This setup can be useful to simulate multiple realizations of a specific non-stationary scenario regardless of its complexity.

In conclusion, the Direct Sampling technique used with the proposed generic setup can produce realistic daily rainfall time-series replicates from different climates without the need of calibration or

additional information. The generality and the total automation of the technique makes it a powerful tool for a routine use in scientific and engineering applications.

Acknowledgements. This research was funded by the Swiss National Science Foundation (project #134614) and supported by the National Centre for ~~Coundwater~~ Groundwater Research and Training (University of New South Wales). The dataset used in this paper is courtesy of the Australian Bureau of Meteorology (BOM).

References

Allard, D., Froidevaux, R., and Biver, P.: Conditional simulation of multi-type non stationary markov object models respecting specified proportions, Mathematical geology, 38, 959–986, 2006.

Arpat, G. and Caers, J.: Conditional simulation with patterns, Mathematical geology, 39, 177–203, 2007.

Bardossy, A. and Plate, E. J.: Space-time model for daily rainfall using atmospheric circulation patterns, Water Resources Research, 28, 1247–1259, doi:10.1029/91WR02589, 1992.

Box, G. E. and Jenkins, G. M.: Time series analysis, control, and forecasting, San Francisco, CA: Holden Day, 1976.

Briggs, W. M. and Wilks, D. S.: Estimating monthly and seasonal distributions of temperature and precipitation using the new CPC long-range forecasts, Journal of Climate, 9, 818–826, doi:10.1175/1520-0442(1996)009<0818:EMASDO>2.0.CO;2, 1996.

Buishand, T. A. and Brandsma, T.: Multisite simulation of daily precipitation and temperature in the Rhine basin by nearest-neighbor resampling, Water Resources Research, 37, 2761–2776, doi:10.1029/2001WR000291, 2001.

Chugunova, T. L. and Hu, L. Y.: Multiple-point simulations constrained by continuous auxiliary data, Mathematical Geosciences, 40, 133–146, doi:10.1007/s11004-007-9142-4, 2008.

Clark, M. P., Gangopadhyay, S., Brandon, D., Werner, K., Hay, L., Rajagopalan, B., and Yates, D.: A resampling procedure for generating conditioned daily weather sequences, Water Resources Research, 40, W04 304, doi:10.1029/2003WR002747, 2004.

Coe, R. and Stern, R. D.: Fitting models to daily rainfall data, Journal of Applied Meteorology, 21, 1024–1031, doi:10.1175/1520-0450(1982)021<1024:FMTDRD>2.0.CO;2, 1982.

Efron, B.: Bootstrap methods - another look at the jackknife, Annals of Statistics, 7, 1–26, doi:10.1214/aos/1176344552, 1979.

Guardiano, F. and Srivastava, R.: Multivariate geostatistics: beyond bivariate moments, Geostatistics-Troia, 1, 133–144, 1993.

Harrold, T. I., Sharma, A., and Sheather, S. J.: A nonparametric model for stochastic generation of daily rainfall occurrence, Water Resources Research, 39, 1300, doi:10.1029/2003WR002182, 2003a.

Harrold, T. I., Sharma, A., and Sheather, S. J.: A nonparametric model for stochastic generation of daily rainfall amounts, Water Resources Research, 39, 1343, doi:10.1029/2003WR002570, 2003b.

Hay, L. E., Mccabe, G. J., Wolock, D. M., and Ayers, M. A.: Simulation of precipitation by weather type analysis, Water Resources Research, 27, 493–501, doi:10.1029/90WR02650, 1991.

Honarkhah, M. and Caers, J.: Stochastic simulation of patterns using distance-based pattern modeling, Mathematical Geosciences, 42, 487–517, 2010.

Hu, L. Y., Liu, Y., Scheepens, C., Shultz, A. W., and Thompson, R. D.: Multiple-Point Simulation with an Existing Reservoir Model as Training Image, Mathematical Geosciences, 46, 227–240, doi:10.1007/s11004-013-9488-8, 2014.

Hughes, J. and Guttorp, P.: A class of stochastic models for relating synoptic atmospheric patterns to regional hydrologic phenomena, Water Resources Research, 30, 1535–1546, 1994.

Hughes, J., Guttorp, P., and Charles, S.: A non-homogeneous hidden Markov model for precipitation occurrence, Journal of the Royal Statistical Society: Series C (Applied Statistics), 48, 15–30, 1999.

Jones, P. G. and Thornton, P. K.: Spatial and temporal variability of rainfall related to a third-order Markov model, Agricultural and Forest Meteorology, 86, 127–138, doi:10.1016/S0168-1923(96)02399-4, 1997.

Kaplan, e. and Meier, p.: Non-parametric estimation from incomplete observations, Journal of the american statistical association, 53, 457–481, doi:10.2307/2281868, 1958.

Katz, R. W. and Parlange, M. B.: Effects of an index of atmospheric circulation on stochastic properties of precipitation, Water Resources Research, 29, 2335–2344, doi:10.1029/93WR00569, 1993.

Katz, R. W. and Zheng, X. G.: Mixture model for overdispersion of precipitation, Journal of Climate, 12, 2528–2537, doi:10.1175/1520-0442(1999)012<2528:MMFOOP>2.0.CO;2, 1999.

Kiely, G., Albertson, J. D., Parlange, M. B., and Katz, R. W.: Conditioning stochastic properties of daily precipitation on indices of atmospheric circulation, Meteorological Applications, 5, 75–87, doi:10.1017/S1350482798000656, http://dx.doi.org/10.1017/S1350482798000656, 1998.

Lall, U. and Sharma, A.: A nearest neighbor bootstrap for resampling hydrologic time series, Water Resources Research, 32, 679–693, doi:10.1029/95WR02966, 1996.

Lall, U., Rajagopalan, B., and Tarboton, D. G.: A nonparametric wet/dry spell model for resampling daily precipitation, Water Resources Research, 32, 2803–2823, doi:10.1029/96WR00565, 1996.

Mariethoz, G. and Renard, P.: Reconstruction of Incomplete Data Sets or Images Using Direct Sampling, Mathematical Geosciences, 42, 245–268, doi:10.1007/s11004-010-9270-0, 2010.

Mariethoz, G., Renard, P., and Straubhaar, J.: The direct sampling method to perform multiple-point geostatistical simulations, Water Resources Research, 46, W11 536, doi:10.1029/2008WR007621, 2010.

Meerschman, E., Pirot, G., Mariethoz, G., Straubhaar, J., Van Meirvenne, M., and Renard, P.: A practical guide to performing multiple-point statistical simulations with the Direct Sampling algorithm, Computers & Geosciences, 52, 307–324, doi:10.1016/j.cageo.2012.09.019, 2013.

Mehrotra, R. and Sharma, A.: A semi-parametric model for stochastic generation of multi-site daily rainfall exhibiting low-frequency variability, Journal of Hydrology, 335, 180–193, doi:10.1016/j.jhydrol.2006.11.011, 2007a.

Mehrotra, R. and Sharma, A.: Preserving low-frequency variability in generated daily rainfall sequences, Journal of Hydrology, 345, 102–120, doi:10.1016/j.jhydrol.2007.08.003, 2007b.

Ndiritu, J.: A variable-length block bootstrap method for multi-site synthetic streamflow generation, Hydrological Sciences Journal, 56, 362–379, doi:10.1080/02626667.2011.562471, 2011.

Rajagopalan, B. and Lall, U.: A k-nearest-neighhor simulator for daily precipitation and other weather variables, Water Resources Research, 35, 3089–3101, doi:10.1029/1999WR900028, 1999.

Sharma, A. and Mehrotra, R.: Rainfall generation, in: Rainfall: state of the science, no. 191 in Geophysical Monograph Series, pp. 215–246, AGU, Washington, D. C., 2010.

Srikanthan, R.: Stochastic generation of daily rainfall data using a nested model, in: 57th Canadian Water Resources Association Annual Congress, pp. 16–18, 2004.

Srikanthan, R.: Stochastic generation of daily rainfall data using a nested transition probability matrix model, in: 29th Hydrology and Water Resources Symposium: Water Capital, 20-23 February 2005, Rydges Lakeside, Canberra, p. 26, Engineers Australia, 2005.

Srikanthan, R. and Pegram, G. G. S.: A nested multisite daily rainfall stochastic generation model, Journal of Hydrology, 371, 142–153, doi:10.1016/j.jhydrol.2009.03.025, 2009.

Srinivas, V. V. and Srinivasan, K.: Hybrid moving block bootstrap for stochastic simulation of multi-site multi-season streamflows, Journal of Hydrology, 302, 307–330, doi:10.1016/j.jhydrol.2004.07.011, 2005.

Straubhaar, J.: MPDS technical reference guide, Centre d'hydrogeologie et geothermie, University of Neuchâtel, 2011.

Straubhaar, J., Renard, P., Mariethoz, G., Froidevaux, R., and Besson, O.: An improved parallel multiple-point algorithm using a list approach, Mathematical Geosciences, 43, 305–328, 2011.

Strebelle, S.: Conditional simulation of complex geological structures using multiple-point statistics, Mathematical Geology, 34, 1–21, 2002.

Tahmasebi, P., Hezarkhani, A., and Sahimi, M.: Multiple-point geostatistical modeling based on the cross-correlation functions, Computational Geosciences, 16, 779–797, 2012.

Vogel, R. M. and Shallcross, A. L.: The moving blocks bootstrap versus parametric time series models, Water Resources Research, 32, 1875–1882, doi:10.1029/96WR00928, 1996.

Wallis, T. W. R. and Griffiths, J. F.: Simulated meteorological input for agricultural models, Agricultural and Forest Meteorology, 88, 241–258, doi:10.1016/S0168-1923(97)00035-X, 1997.

Wang, Q. J. and Nathan, R. J.: A daily and monthly mixed algorithm for stochastic generation of rainfall time series, in: Water Challenge: Balancing the Risks: Hydrology and Water Resources Symposium 2002, p. 698, Institution of Engineers, Australia, 2002.

Wilby, R. L.: Modelling low-frequency rainfall events using airflow indices, weather patterns and frontal frequencies, Journal of Hydrology, 212, 380–392, doi:10.1016/S0022-1694(98)00218-2, 1998.

Wilks, D. S.: Conditioning stochastic daily precipitation models on total monthly precipitation, Water Resources Research, 25, 1429–1439, doi:10.1029/WR025i006p01429, 1989.

Wojcik, R. and Buishand, T. A.: Simulation of 6-hourly rainfall and temperature by two resampling schemes, Journal of Hydrology, 273, 69–80, doi:10.1016/S0022-1694(02)00355-4, 2003.

Wojcik, R., McLaughlin, D., Konings, A., and Entekhabi, D.: Conditioning stochastic rainfall replicates on remote sensing data, IEEE T. Geosci. Remote, 47, 2436–2449, 2009.

Woolhiser, D. A., Keefer, T. O., and Redmond, K. T.: Southern oscillation effects on daily precipitation in the southwestern United-States, Water Resources Research, 29, 1287–1295, doi:10.1029/92WR02536, 1993.

Young, K. C.: A multivariate chain model for simulating climatic parameters from daily data, Journal of Applied Meteorology, 33, 661–671, doi:10.1175/1520-0450(1994)033<0661:AMCMFS>2.0.CO;2, 1994.

Zhang, T., Switzer, P., and Journel, A.: Filter-based classification of training image patterns for spatial simulation, Math. Geol., 38, 63–80, 2006.

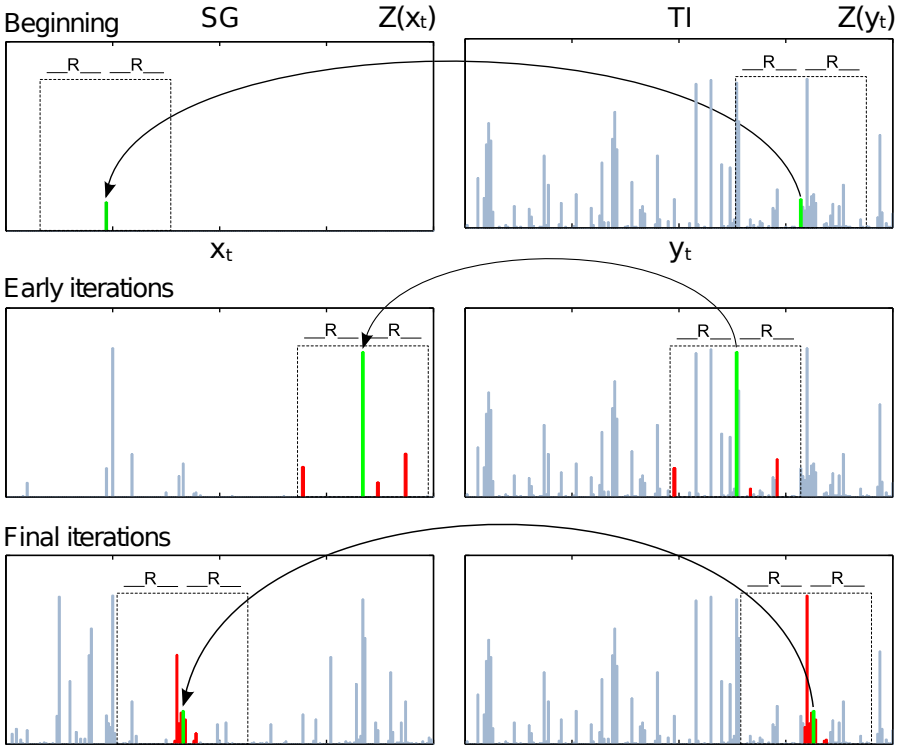

Fig. 1. Sketch of ~~a~~ the sequential simulation of a rainfall time-series performed by the Direct Sampling: the ~~chain represents the SG, with circles corresponding to uninformed time steps and full dots denoting simulated data. The~~ dashed rectangle represents the search neighborhood of radius R, the datum being simulated is ~~indicated with the arrow~~ in green and the ones composing the data event are ~~numbered~~in red. ~~In this example, $R = 6$~~ Note the non-exact match between the data event in the SG and the ~~maximum number of neighbors $N = 4$~~one in the TI.

Table 1. Summary of the ~~used~~ dataset used.

Location	Station	Period [years]	Record length [days]	Missing data [days]
Alice Springs	A.S.Airport	1940-2013	26347	305
Sydney	S.Observatory Hill	1858-2013	56662	184
Darwin	D.Airport	1941-2013	26356	0

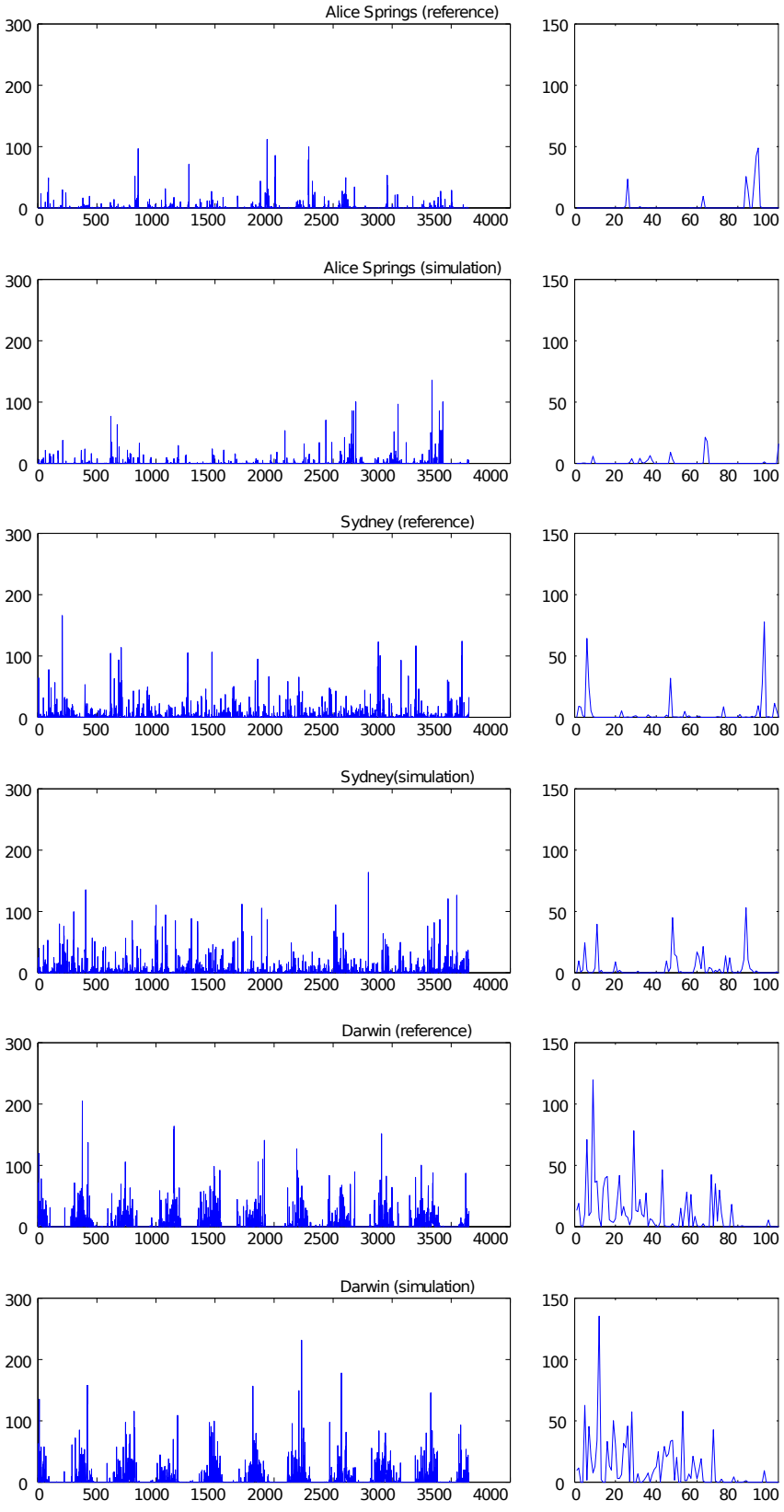

Fig. 2. Visual comparison between the simulated and the reference daily rainfall [mm] time-series: 10-years (left column) and 100-days (right column) random samples.

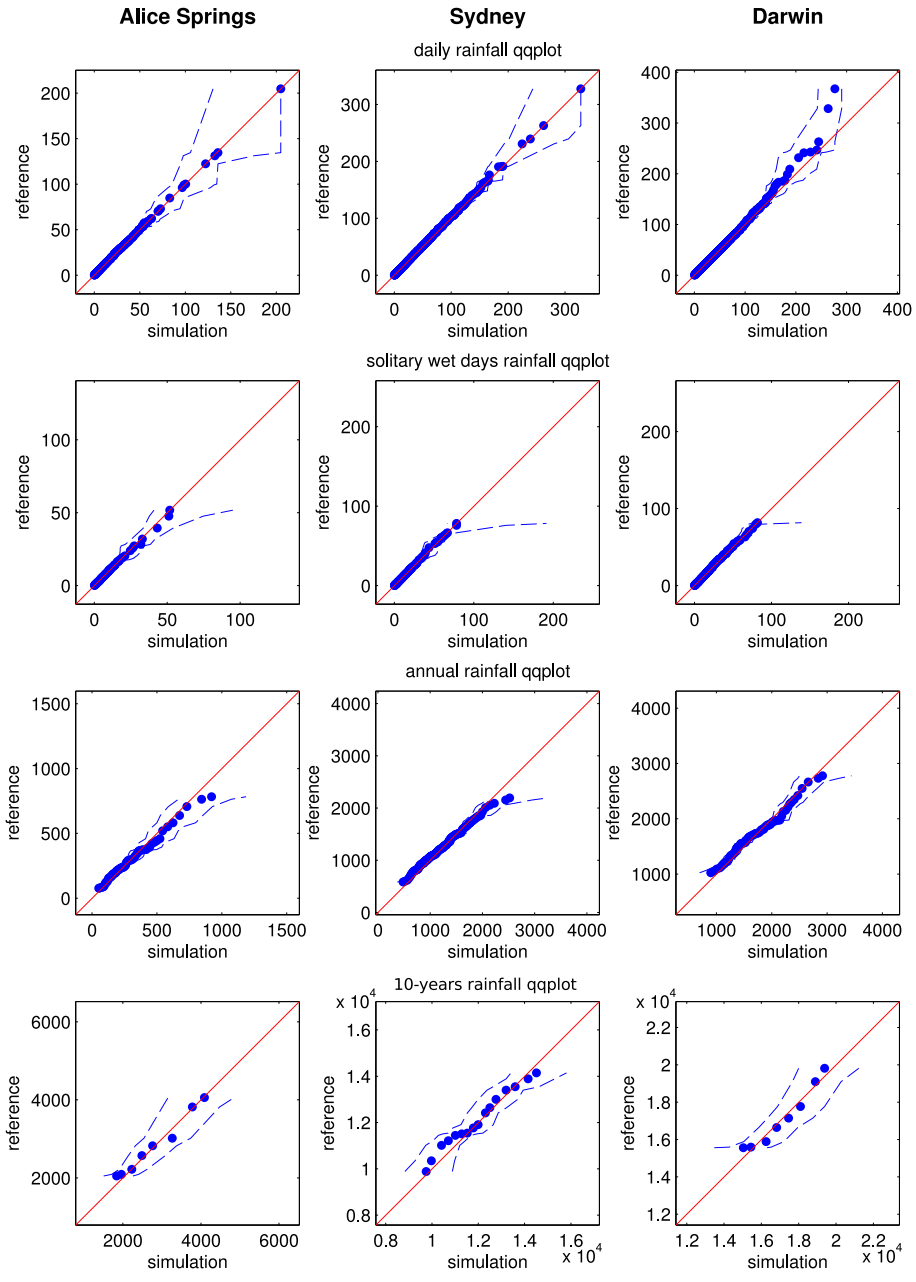

Fig. 3. qq-plots of the empirical probability rainfall amount [mm] distributions: median of the realizations (~~dotted line~~blue dots), 5th and 95th percentile (dashed lines). The bisector (solid line) indicates the exact quantile match.

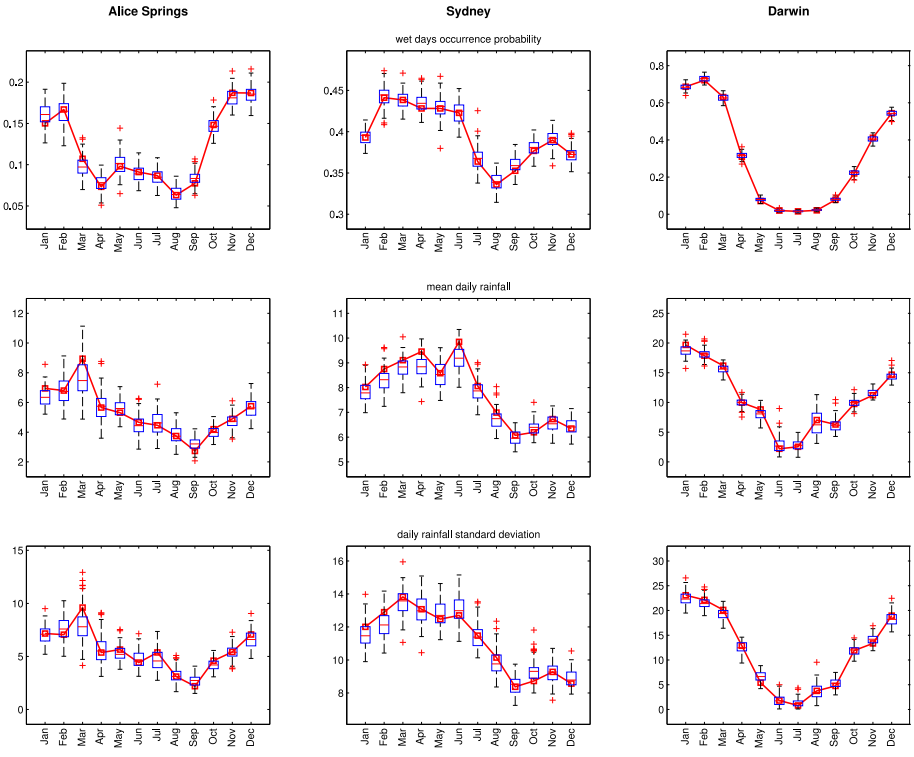

Fig. 4. Box-plots of the average wet days probability, mean daily rainfall amount [mm] and its standard deviation per month. The solid line indicates the reference.

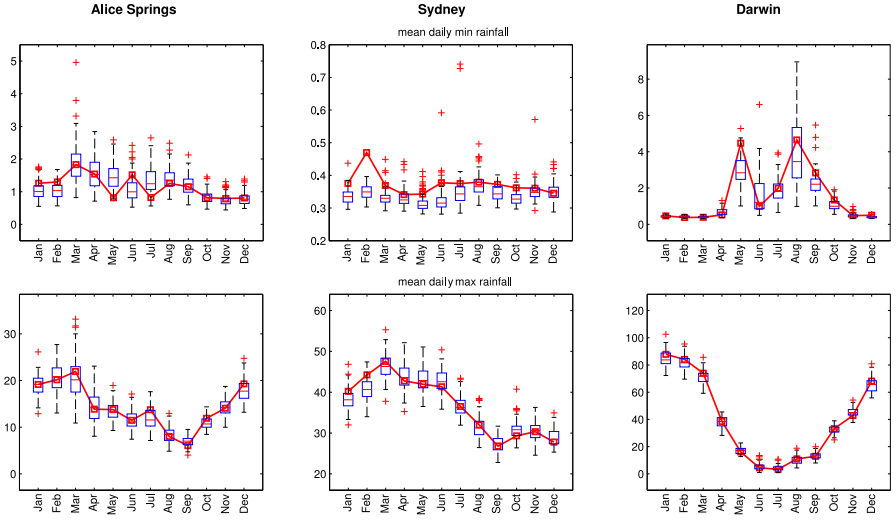

Fig. 5. Box-plots of the average extremes per month [mm]. The solid line indicates the reference.

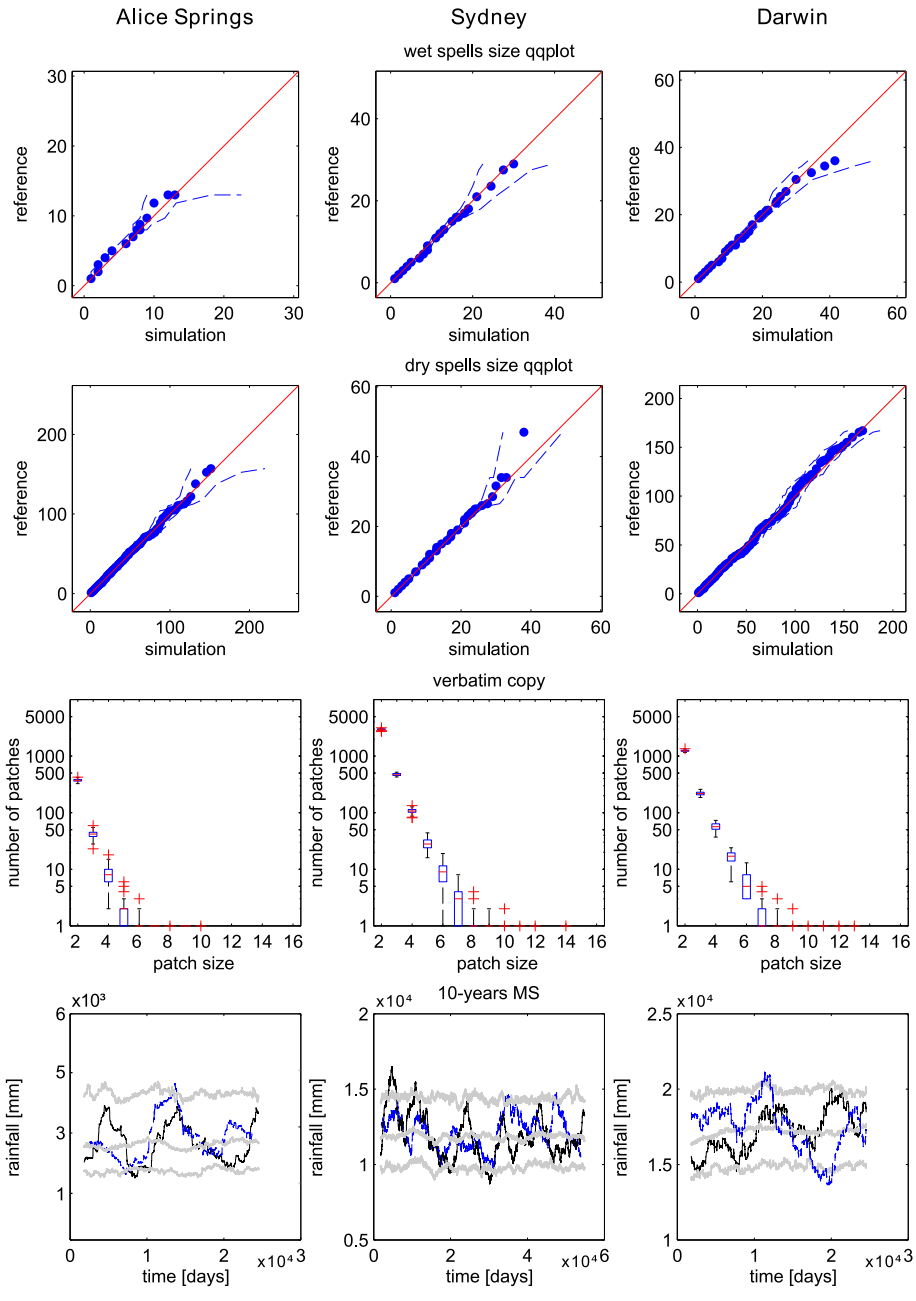

Fig. 6. Main indicators describing the rainfall pattern: qq-plots of the dry and wet spells [days] distributions, verbatim copy box-plots as function of the patch size [days] and daily 10-years Moving Sum (MS) time-series [mm] of the reference (black line), median, 5-th and 95-th percentile of the realizations (gray lines) and a randomly picked simulation (dashed blue line).

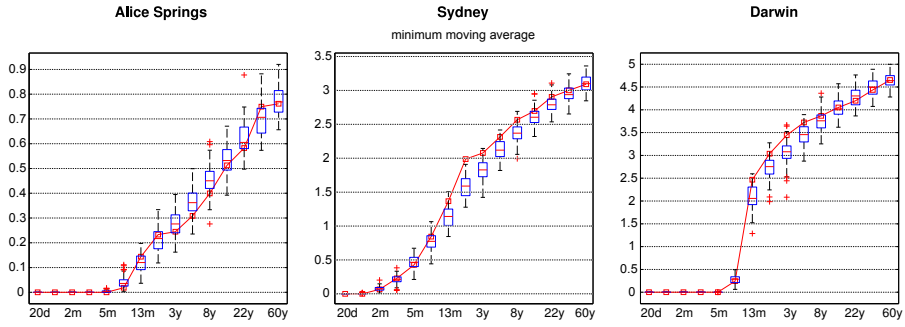

Fig. 7. ~~Sample Partial Autocorrelation Function (PACF)~~ Minimum moving average of ~~the~~ daily ~~, monthly and annual~~ rainfall ~~signal: the reference~~ [mm] for different running window lengths (~~solid line)~~days, ~~100 DS simulations (box-plots~~months or years)~~, and confidence bounds for~~ . The solid line indicates the ~~negligible autocorrelation indexes (dashed lines)~~reference.

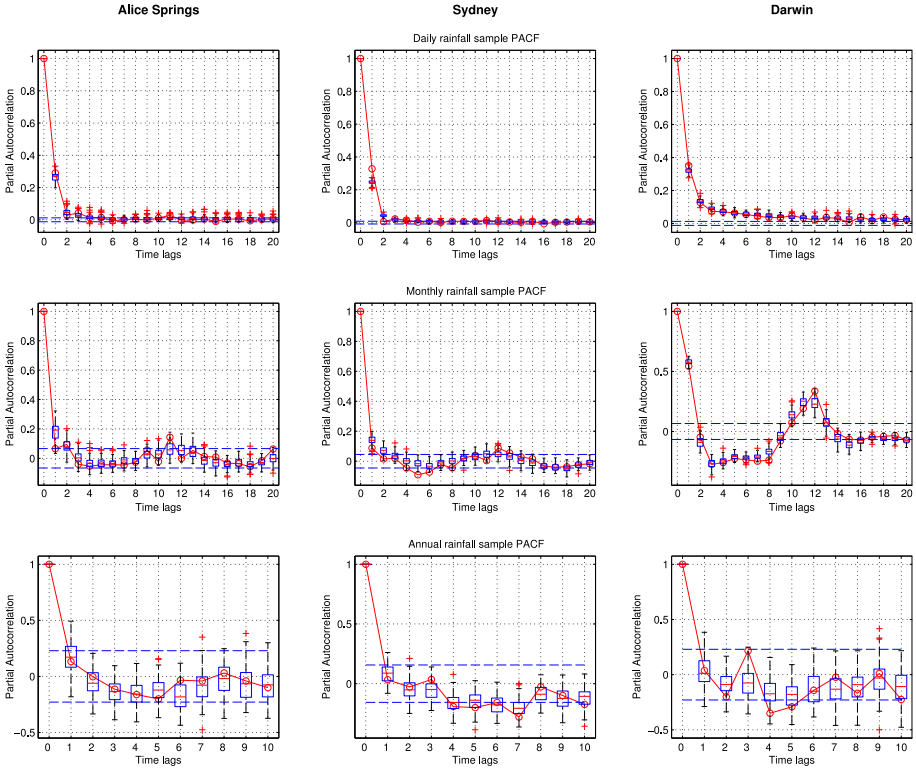

Fig. 8. Sample Partial Autocorrelation Function (PACF) of the daily, monthly and annual rainfall signal: the reference (solid line), 100 DS simulations (box-plots), and confidence bounds for the negligible autocorrelation indexes (dashed lines).

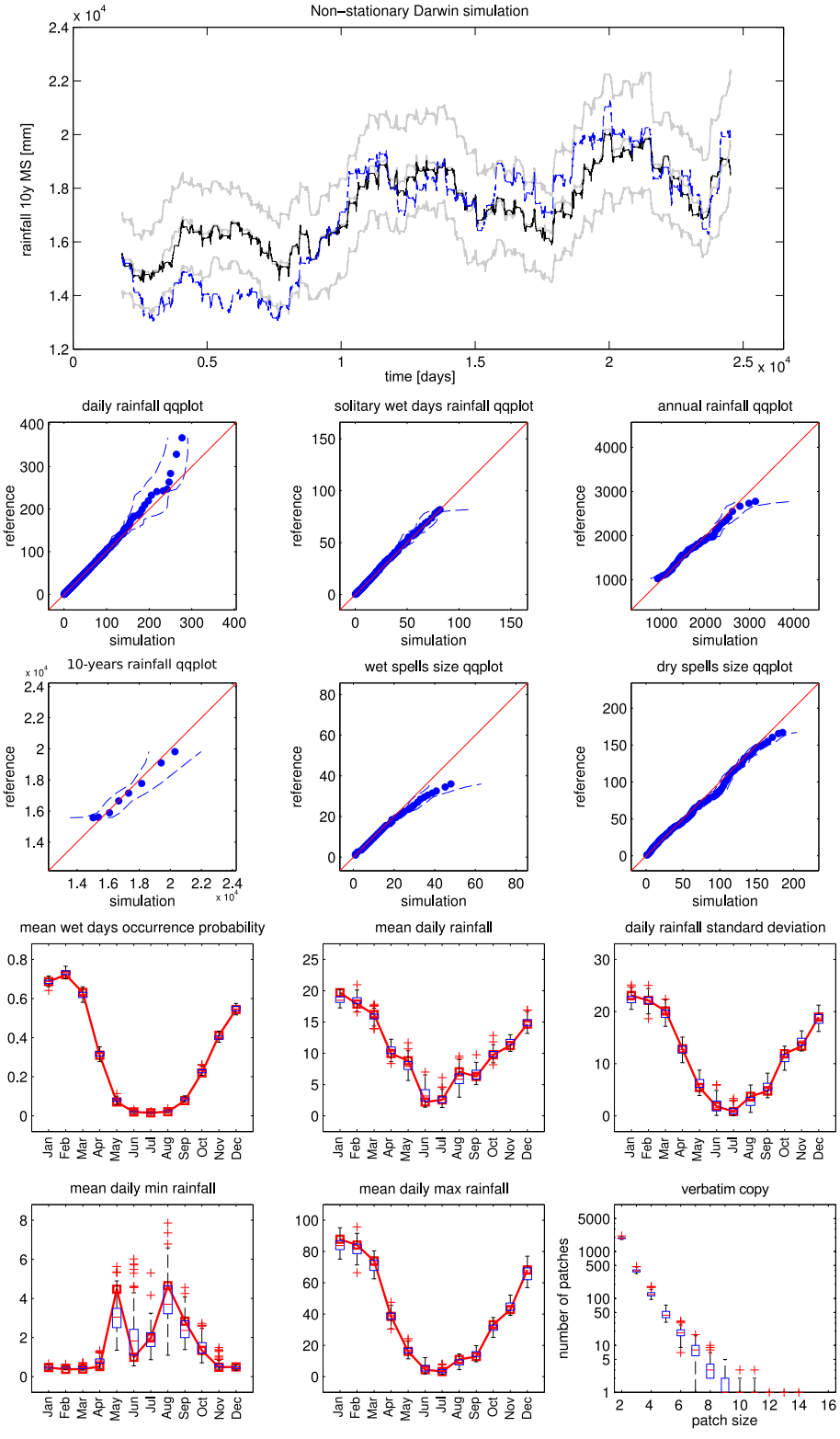

Fig. 9. Darwin daily rainfall non-stationary simulation: 10-years Moving Sum time-series (top) of the reference (black line), median, 5-th and 95-th percentile of the realizations (gray lines) and a randomly picked simulation (dashed blue line); main quantile-comparisons (center), main seasonal indicators and verbatim copy box-plot (bottom).

Table 2. Standard setup proposed for rainfall simulation. The parameters are: search window radius R, maximum number of neighbors N and distance threshold T. The variables are: 1) the 365 days Moving Average ($365MA$), 2) the Moving Sum of the current day and the one before ($2MS$), 3) and 4) annual seasonality triangular functions ($tr1$ and $tr2$), 5) the dry/wet sequence dw and 6) the daily rainfall amount as the target variable. On the right, a portion of multivariate TI is given as example.

Variable	R	N	T	
1) $365MA$	5000	21	0.05	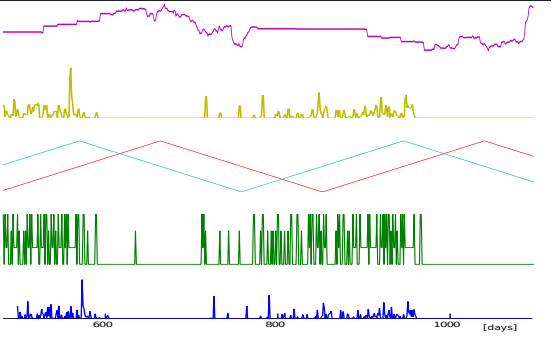
2) $2MS$	1	1	0.05	
3) $tr1$	1	1	0.05	
4) $tr2$	1	1	0.05	
5) dw	10	5	0.05	
6) $rainfall$	5000	21	0.05	